

PAPER • OPEN ACCESS

Cosmological global dynamical systems analysis

To cite this article: Artur Alho *et al* 2022 *Class. Quantum Grav.* **39** 145010

View the [article online](#) for updates and enhancements.

You may also like

- [Mathematics Modeling of Diabetes Mellitus Type SEII₊ by Considering Treatment and Genetics Factors](#)
Asmaidi and Eka Dodi Suryanto
- [An improved measurement of dsDNA elasticity using AFM](#)
Thi-Huong Nguyen, Sang-Myung Lee, Kyoungwan Na et al.
- [Neural networks that use three-state neurons](#)
J S Yedidia

Cosmological global dynamical systems analysis

Artur Alho^{1,*} , Woei Chet Lim²  and Claes Uggle³ 

¹ Center for Mathematical Analysis, Geometry and Dynamical Systems, Instituto Superior Técnico, Universidade de Lisboa, Av. Rovisco Pais, 1049-001 Lisboa, Portugal

² Department of Mathematics, University of Waikato, Private Bag 3105, Hamilton 3240, New Zealand

³ Department of Physics, Karlstad University, S-65188 Karlstad, Sweden

E-mail: aalho@math.ist.utl.pt and wclim@waikato.ac.nz

Received 28 January 2022, revised 16 May 2022

Accepted for publication 9 June 2022

Published 29 June 2022



Abstract

We consider a dynamical systems formulation for models with an exponential scalar field and matter with a linear equation of state in a spatially flat and isotropic spacetime. In contrast to earlier work, which only considered linear hyperbolic fixed point analysis, we do a center manifold analysis of the non-hyperbolic fixed points associated with bifurcations. More importantly though, we construct monotonic functions and a Dulac function. Together with the complete local fixed point analysis this leads to proofs that describe the entire global dynamics of these models, thereby complementing previous local results in the literature.

Keywords: cosmology, dynamical systems, global dynamics, scalar field, perfect fluid

1. Introduction

Dynamical systems and dynamical systems methods were introduced in cosmology in 1971 by Collins [1] who treated two-dimensional dynamical systems while Bogoyavlensky and Novikov (1973) [2] used dynamical systems techniques for higher dimensional dynamical systems in cosmology. This early work has subsequently been followed up and extended by many researchers, see e.g. [3–5]. The first dynamical systems analysis involving a minimally coupled scalar field was given by Belinskii and co-workers [6–9] who used dynamical systems to explore inflation, primarily focusing on the potentials $V(\varphi) = \frac{1}{2}m^2\varphi^2$ and $V(\varphi) = \frac{1}{4}\lambda(\varphi^2 - \varphi_0^2)^2$. In 1987 Halliwell [10] treated an exponential scalar field potential in Friedmann–Lemaître–Robertson–Walker (FLRW) cosmology, where the scalar field and an

*Author to whom any correspondence should be addressed.



exponential representation of the cosmological scale factor were used as dynamical systems variables, which resulted in an unbounded state space and thereby only a local state space description [see also Ratra and Peebles (1988) [11] for early work using dynamical systems for this case]. The first global state space treatment of a scalar field with an exponential potential was done in Bianchi cosmology, which contains FLRW cosmology as a special case, by Coley *et al* (1997) [12]. Notable is also the work by Foster (1998) [13] who analysed asymptotically exponential scalar field potentials. Finally, Copeland *et al* (1998) [14] treated the spatially flat FLRW case with an exponential potential and a perfect fluid with a linear equation of state. This latter work, which used a reduced two-dimensional compact and regular state space, gave a linear fixed point (critical point, equilibrium point) stability analysis for parameter values that yielded hyperbolic fixed points⁴.

In this paper we will investigate the models Copeland *et al* considered, but we will extend their local fixed point analysis to the bifurcation values of the relevant model parameters, which yield non-hyperbolic fixed points with one zero eigenvalue, thereby requiring center manifold analysis. More importantly though, even in the case of the hyperbolic fixed points a linear fixed point analysis in a two-dimensional compact state space does not necessarily imply a complete asymptotic description; other asymptotic behavior is possible, such as periodic orbits and heteroclinic cycles⁵. In this paper we fill these gaps in the proof for the asymptotic and global behavior of models with an exponential scalar field potential and a perfect fluid with a linear equation of state.

We finally note three additional motivational points: first, an exponential potential is no longer considered to be suitable for describing inflation and/or quintessence. For this reason there is a plethora of different scalar field potentials in the literature. A substantial fraction of these potentials are asymptotically exponential when the scalar field $\varphi \rightarrow +\infty$ or/and $\varphi \rightarrow -\infty$. We are presently investigating FLRW models with perfect fluids and asymptotically exponential potentials, and perturbations thereof, by means of new regular and bounded state space descriptions where the models in this paper appear as invariant boundaries. Due to this, global analytical and systematic numerical results for these more general and physically interesting models *require* a global understanding of the present ones.

Second, the present FLRW models also appear as invariant subsets of more geometrically general models, such as anisotropic spatially homogeneous models and hypersurface self-similar models, e.g., spherically symmetric ones, relevant for black hole formation, see e.g. [16–19], and references therein. A global understanding of these more general models therefore again requires a full understanding of the present ones. This even holds for asymptotic features of models with no symmetries at all, since the present models appear as special invariant sets on the so-called local boundary, which describes isotropic singularities and some of the aspects of general spacelike singularities, see e.g. [20, 21]. Furthermore, by combining these first two motivational points, the present models form part of the picture for even more general situations. The global results in this paper thereby constitute an important foundation for studies of a very broad range of physically interesting problems.

⁴ All eigenvalues of a linearization of a dynamical system at a so-called hyperbolic fixed point have non-zero real parts, and hence such a fixed point has no center manifolds.

⁵ A heteroclinic orbit is a solution trajectory that originates and ends at two different fixed points; a heteroclinic chain consists of a concatenation of heteroclinic orbits, where the ending fixed point of one heteroclinic orbit is the starting fixed point of the next one; a heteroclinic cycle is a closed heteroclinic chain. For an example and detailed discussion of a heteroclinic cycle arising from a scalar field potential in the spatially flat FLRW case, see Foster (1998) [15].

Third, a key ingredient for several of the proofs in the present paper are monotonic functions, which are *derived* by using methods first developed by Uggla in chapter 10 in [3] and later generalized by Uggla and co-workers in [22, 23]. The present results thereby serve as an illustration of the power and use of those methods, which can be applied to a plethora of currently popular topics, e.g., a wide range of problems in cosmology and astrophysics in both general relativity and various modified gravity theories, when the corresponding equations are properly reformulated into useful dynamical systems.

2. Dynamical systems description and local fixed point analysis

2.1. Field equations

We consider a flat and isotropic FLRW spacetime,

$$ds^2 = -dt^2 + a^2(t)\delta_{ij}dx^i dx^j, \quad (1)$$

where $a(t)$ is the cosmological scale factor. The source consists of matter with an energy density $\rho_{\text{pf}} > 0$ and pressure p_{pf} , and a minimally coupled scalar field, φ , with a potential $V(\varphi) > 0$, which results in

$$\rho_\varphi = \frac{1}{2}\dot{\varphi}^2 + V(\varphi), \quad p_\varphi = \frac{1}{2}\dot{\varphi}^2 - V(\varphi). \quad (2)$$

The Einstein equations, the (non-linear) Klein–Gordon equation, and the energy conservation law for the fluid, are given by⁶ (see, e.g., [24] for a slightly different formulation of the equations)

$$\dot{a} = aH, \quad (3a)$$

$$\dot{H} + H^2 = -\frac{1}{6}(\rho + 3p), \quad (3b)$$

$$3H^2 = \rho, \quad (3c)$$

$$\ddot{\varphi} = -3H\dot{\varphi} - V_{,\varphi}, \quad (3d)$$

$$\dot{\rho}_{\text{pf}} = -3H\gamma\rho_{\text{pf}}, \quad (3e)$$

where an overdot represents the derivative with respect to the cosmic time t ; a barotropic equation of state for the perfect fluid yields $\gamma = \gamma(\rho_{\text{pf}})$; the total energy density ρ and pressure p are given by

$$\rho = \rho_\varphi + \rho_{\text{pf}}, \quad p = p_\varphi + p_{\text{pf}}. \quad (4)$$

Equation (3b) is the (Landau–) Raychaudhuri equation, while (3c) is the Gauss/Hamiltonian constraint (often referred to as the Friedmann equation in FLRW cosmology). Here we are going to consider an exponential potential and a perfect fluid with a linear equation of state, i.e.,

$$V = V_0 e^{-\lambda\varphi}, \quad p_{\text{pf}} = (\gamma - 1)\rho_{\text{pf}}, \quad (5)$$

where λ and γ are constants; matter, radiation and a stiff perfect fluid correspond to $\gamma = 1$, $\gamma = 4/3$ and $\gamma = 2$, respectively.

⁶ We use units such that $c = 1$ and $8\pi G = 1$, where c is the speed of light and G is Newton's gravitational constant.

2.2. Explicitly solvable cases

For an exponential potential and a perfect fluid with linear equation of state the equations are solvable for several values of λ and γ , as was shown implicitly by Uggla *et al* (1995) [19] (use equations (2.23), (2.37), (4.98) and $\varphi = \sqrt{6}\beta^\dagger$ in table III in [19]), where it was also demonstrated how to obtain explicit solutions in as simple form as possible⁷. The solvable cases are:

$$\lambda = 0, \quad \gamma = 2, \quad (6a)$$

$$\lambda = \pm\sqrt{6}(\gamma - 1), \quad \lambda = \pm\left(\frac{10 + \gamma}{2\sqrt{6}}\right), \quad \lambda = \pm\sqrt{\frac{3}{2}}\gamma, \quad (6b)$$

$$\lambda = \pm\sqrt{\frac{3}{2}}(4 - 3\gamma), \quad \lambda = \pm\left(\frac{4 + \gamma}{\sqrt{6}}\right), \quad (6c)$$

where we recognize the first case, $\lambda = 0$, as a constant potential and the second case, $\gamma = 2$, as a stiff perfect fluid⁸. A problem where either the scalar field potential, V , or ρ_{pf} is zero yields a trivially solvable problem, see [19].

2.3. The dynamical system

To obtain a useful dynamical system, we introduce the following *dimensionless bounded* quantities⁹

$$\Sigma_\varphi \equiv \frac{\dot{\varphi}}{\sqrt{6}H} = \frac{\varphi'}{\sqrt{6}}, \quad (7a)$$

$$\Omega_V \equiv \frac{V}{3H^2}, \quad (7b)$$

$$\Omega_{\text{pf}} \equiv \frac{\rho_{\text{pf}}}{3H^2}. \quad (7c)$$

A' henceforth denotes the derivative with respect to e -fold time

$$N \equiv \ln a/a_0, \quad (8)$$

where $a_0 = a(t_0)$, $t = t_0 \Rightarrow N = 0$. The definition (8) implies that $N \rightarrow -\infty$ and $N \rightarrow +\infty$ when $a \rightarrow 0$ and $a \rightarrow \infty$, respectively.

Throughout we replace t with N by using that

$$\frac{d}{dt} = H \frac{d}{dN}, \quad \frac{d^2}{dt^2} = H^2 \left(\frac{d^2}{dN^2} - (1 + q) \frac{d}{dN} \right), \quad (9)$$

⁷ To the authors' knowledge, all known explicit solutions for problems with hypersurface homogeneity, in general relativity and modified gravity theories, are obtainable, and in their simplest form, by using the mechanisms and methods in [19].

⁸ The explicitly solvable case $\gamma = 1$, $\lambda = \sqrt{3/2}$ was used in [24] to illustrate how explicit solutions can be situated in a dynamical systems context.

⁹ The variable Σ_φ was first introduced by Coley *et al* (1997) [12] and Copeland *et al* (1998) [14] whose x is Σ_φ . Since then, Σ_φ (or φ') is often used to describe scalar fields in cosmology, see, e.g., Ureña-López (2012) [25], equation (2.3), Tsujikawa (2013) [26], equation (16) and Alho and Uggla (2015) [24], equation (8). The reason for using the notation Σ for the kernel is because Σ_φ plays a similar role as Hubble-normalized shear, which is typically denoted with the kernel Σ , see e.g. [3].

where

$$q \equiv -\frac{a\ddot{a}}{\dot{a}^2} = -1 - \frac{H'}{H} \quad (10)$$

is the *deceleration parameter*.

Using N and inserting (5) and the definitions (7) into (3) results in the following coupled system for the state vector $(\Sigma_\varphi, \Omega_{\text{pf}})$:

$$\Sigma'_\varphi = -(2 - q)\Sigma_\varphi + \sqrt{\frac{3}{2}}\lambda\Omega_V, \quad (11a)$$

$$\Omega'_{\text{pf}} = [2(1 + q) - 3\gamma]\Omega_{\text{pf}}, \quad (11b)$$

where

$$\Omega_V = 1 - \Sigma_\varphi^2 - \Omega_{\text{pf}}, \quad (12a)$$

$$q = -1 + 3\Sigma_\varphi^2 + \frac{3}{2}\gamma\Omega_{\text{pf}} = 2 - 3\Omega_V - \frac{3}{2}(2 - \gamma)\Omega_{\text{pf}}. \quad (12b)$$

Restricting γ to $\gamma \in (0, 2)$, as we will do later, it follows that $-1 \leq q \leq 2$, where $q = -1$ when $\lambda = 0$ and $\Sigma_\varphi = \Omega_{\text{pf}} = 0$, while $q = 2$ when $\Sigma_\varphi = \pm 1$, $\Omega_{\text{pf}} = 0$. Another quantity that is often used in the context of scalar field is $w_\varphi \equiv p_\varphi/\rho_\varphi$, or, equivalently, γ_φ , defined by $p_\varphi = (\gamma_\varphi - 1)\rho_\varphi$ and hence

$$\gamma_\varphi \equiv \frac{p_\varphi + \rho_\varphi}{\rho_\varphi} = \frac{2\Sigma_\varphi^2}{1 - \Omega_{\text{pf}}}. \quad (13)$$

We use (12a) in (11) to globally solve for Ω_V , although note that

$$\Omega'_V = 2 \left(1 + q - \sqrt{\frac{3}{2}}\lambda\Sigma_\varphi \right) \Omega_V, \quad (14)$$

which follows from (12a) and (11). This equation and (11b) show that $\Omega_V = 0$ and $\Omega_{\text{pf}} = 0$ form an invariant boundary of the state space $(\Sigma_\varphi, \Omega_{\text{pf}})$, which, due to that the dynamical system (11) is completely regular, can be included in the state space analysis. This is essential since some of the asymptotics are associated with this boundary. We will refer to the orbits with $\Omega_V > 0$, $\Omega_{\text{pf}} > 0$ as *interior orbits* and orbits with $\Omega_V = 1 - \Sigma_\varphi^2 - \Omega_{\text{pf}} = 0$ or/and $\Omega_{\text{pf}} = 0$, as boundary orbits.

The present formulation can be viewed as a transformation of an original state space $(H, \rho_{\text{pf}}, \dot{\varphi}, \varphi)$ (alternatively, $(H, a, \dot{\varphi}, \varphi)$, since $\rho_{\text{pf}} \propto a^{-3\gamma}$) to $(H, \varphi, \Sigma_\varphi, \Omega_{\text{pf}})$. The equations for H and φ , $H' = -(1 + q)H$ and $\varphi' = \sqrt{6}\Sigma_\varphi$, decouple from the dynamical system for $(\Sigma_\varphi, \Omega_{\text{pf}})$. This reduced state space can be therefore be regarded as a projection of the state space $(H, \varphi, \Sigma_\varphi, \Omega_{\text{pf}})$.¹⁰ The reason for the decoupling of H and φ is due to the linear equation of state for the perfect fluid and that $-V_{,\varphi}/V = \lambda = \text{constant}$ ¹¹. Since the decoupled equations

¹⁰ More precisely, the new variables result in a skew-product dynamical system where the base dynamics acts in $(\Sigma_\varphi, \Omega_{\text{pf}})$ while the fiber dynamics acts in (H, φ) , a notion that was introduced in [27].

¹¹ The present system is closely connected to that of Copeland *et al* (1998) [14] who used $x = \Sigma_\varphi$ and $y = \sqrt{\Omega_V}$ as variables. We prefer to use the more physical variable Ω_{pf} rather than y . Moreover, note that in contrast to Ω_{pf} , the unfortunately widely used y is unsuitable for many more general potentials. For examples where y is inappropriate and for proper choices of variables, see, e.g., [28–31].

Table 1. Fixed points and their effective scalar field equation of state γ_φ ; deceleration parameter q ; their eigenvalues, where $r \equiv 1 - \frac{8\gamma(\lambda^2-3\gamma)}{\lambda^2(2-\gamma)} = \frac{24\gamma^2-(9\gamma-2)\lambda^2}{\lambda^2(2-\gamma)}$.

Name	Σ_φ	Ω_{pf}	γ_φ	q	Eigenvalues
K_+	1	0	2	2	$3(2-\gamma); \sqrt{6}(\sqrt{6}-\lambda)$
K_-	-1	0	2	2	$3(2-\gamma); \sqrt{6}(\sqrt{6}+\lambda)$
P/dS	$\frac{\lambda}{\sqrt{6}}$	0	$\frac{\lambda^2}{3}$	$\frac{1}{2}(\lambda^2-2)$	$-\frac{1}{2}(6-\lambda^2); -(3\gamma-\lambda^2)$
FL	0	1	—	$\frac{1}{2}(3\gamma-2)$	$3\gamma; -\frac{3}{2}(2-\gamma)$
S	$\sqrt{\frac{3}{2}}\left(\frac{\lambda}{\lambda}\right)$	$1 - \frac{3\gamma}{\lambda^2}$	γ	$\frac{1}{2}(3\gamma-2)$	$-\frac{3}{4}(2-\gamma)(1 \pm \sqrt{r})$

can be solved by quadratures once $\Sigma_\varphi(N)$ and $\Omega_{\text{pf}}(N)$ are obtained, the system for the state vector $(\Sigma_\varphi, \Omega_{\text{pf}})$ contains the essential information for the present problem.

2.4. Local hyperbolic fixed point analysis

The fixed points of the dynamical system (11) and the eigenvalues of the linearization at the fixed points are given in table 1.

The names of the fixed points are motivated as follows: K_\pm are the boundary ‘kinaton’ fixed points, due to that $\Omega_V = 0$ and $\Omega_{\text{pf}} = 0$ and hence that $H' = -(1+q)H = -3H \Rightarrow 3H^2 = \rho = \rho_\varphi = 3H_0^2 \exp(-6N) = 3H_0^2(a_0/a)^6$, which characterizes kinaton evolution (a nomenclature introduced in [32]); dS with $\lambda = 0$ and $q = -1$ is the de Sitter fixed point while P, which exists when $0 < \lambda^2 < 6$ and yields power law acceleration when $\lambda^2 < 2$, due to that $q = (\lambda^2 - 2)/2$ at P; the fixed point FL is referred to as the Friedmann–Lemaître fixed point ($\Omega_{\text{pf}} = 1$); finally S is the scaling fixed point (scaling due that $\gamma_\varphi = \gamma$ at S, since this implies that the scalar field mimics the dynamics of the fluid, with a constant ratio between both energy densities).

Apart from the de Sitter fixed point dS, which exists when $\lambda = 0$, each of the other fixed points correspond to a unique self-similar (i.e., the corresponding spacetime admits a homothetic Killing vector field) power law solution, invariant under constant conformal scalings. On the other hand, the de Sitter fixed point dS corresponds to a one-parameter set of solutions, parametrized by the dimensional constant $V_0 = \Lambda = 3H_0^2$.

Without loss of generality, we will assume that $\lambda \geq 0$ (if $\lambda < 0$, make the change $\varphi \rightarrow -\varphi$). We also limit the range of γ so that $\gamma \in (0, 2)$ where $\gamma = 0$ and $\gamma = 2$ yield bifurcations, which is not surprising since $\gamma = 0$ results in a cosmological constant while a stiff fluid equation of state, $\gamma = 2$, corresponds to that the speed of sound is equal to that of light (also, recall that $\gamma = 2$ is an explicitly solvable case). The above eigenvalues then yield the stability properties given in table 2.

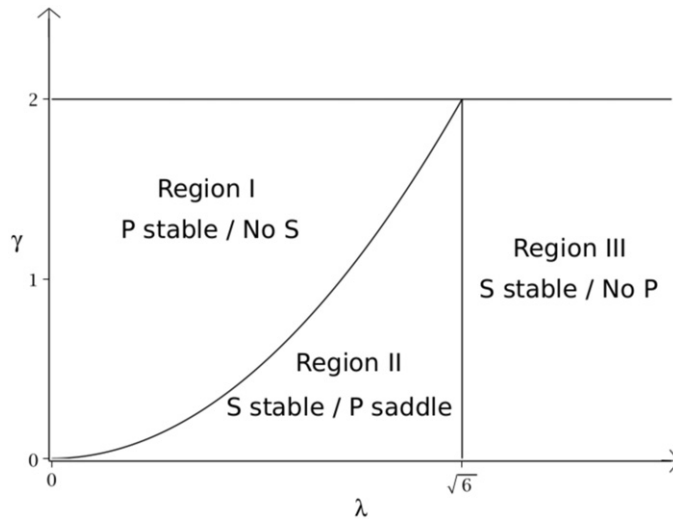
It follows that there are three disjoint parameter regions when $\gamma \in (0, 2)$, $\lambda \geq 0$, determined by the two bifurcations at $\gamma = \lambda^2/3$ and $\lambda = \sqrt{6}$, see figure 1:

- I $\gamma > \lambda^2/3$.
- II $\gamma < \lambda^2/3$, $\lambda < \sqrt{6}$.
- III $\lambda > \sqrt{6}$.

The $\lambda = 0$ boundary of region I, where the stable fixed point P is replaced with the stable fixed point dS is, as mentioned, completely solvable. The solution in the state space $(\Sigma_\varphi, \Omega_{\text{pf}})$ can be obtained as follows. In this case, due to that $\lambda = 0$, the system (11) is invariant under $\Sigma_\varphi \rightarrow -\Sigma_\varphi$. Hence Σ_φ can be replaced with $\Sigma_\varphi^2 = \Omega_{\text{stiff}}$. This results in a system that is identical to that for a source with three matter components: (i) a perfect fluid with

Table 2. Fixed points and their stability; $\gamma \in (0, 2)$.

Name	Domain	Stability
K_+	$\lambda \geq 0$	Unstable node when $\lambda < \sqrt{6}$
K_-	$\lambda \geq 0$	Saddle point for $\lambda > \sqrt{6}$
P/dS	$0 \leq \lambda^2 < 6$	Unstable node
FL	$\lambda \geq 0$	Stable node when $\lambda^2 < 3\gamma$
		Saddle point for $3\gamma < \lambda^2 < 6$
S	$\lambda^2 > 3\gamma$	Saddle point
		Stable node when $3\gamma < \lambda^2 < \frac{24\gamma^2}{9\gamma-2}$
		Stable spiral for $\lambda^2 > \frac{24\gamma^2}{9\gamma-2}$

**Figure 1.** Bifurcation diagram (γ, λ) .

$p_{\text{pf}} = (\gamma_{\text{pf}} - 1)\rho_{\text{pf}}$, (ii) a stiff fluid, i.e., a perfect fluid with an equation of state $p_{\text{stiff}} = \rho_{\text{stiff}}$ (and hence $\rho'_{\text{stiff}} = -6\rho_{\text{stiff}}$), and (iii) a cosmological constant, $\Lambda = V$. This problem easily yields the solution

$$(\Omega_{\text{stiff}}, \Omega_{\text{pf}}) = \frac{(\Omega_{\text{stiff},0} e^{-6N}, \Omega_{\text{pf},0} e^{-3\gamma N})}{\Omega_{\text{stiff},0} e^{-6N} + \Omega_{\text{pf},0} e^{-3\gamma N} + \Omega_{V,0}}, \quad (15)$$

while $\Sigma_\varphi = \pm\sqrt{\Omega_{\text{stiff}}}$ and $\Omega_V = 1 - \Omega_{\text{stiff}} - \Omega_{\text{pf}}$. The invariant subset $\Sigma_\varphi = 0$, and hence $\Omega_{\text{stiff}} = 0$, corresponds to having a perfect fluid with a linear equation of state and a cosmological constant, where $\gamma = 1$ yields the Λ CDM model. For a visual representation of the orbit structure for the $\lambda = 0$ models, see figure 2.

The bifurcation boundary between region I and II at $\gamma = \lambda^2/3$ corresponds to that S enters the state space through P and takes over as the stable sink when $\gamma < \lambda^2/3$ instead of P, which is a stable sink in region I and a saddle with one orbit entering the interior of the state space in region II. The bifurcation boundary between regions II and III at $\lambda = \sqrt{6}$ corresponds to that P leaves the state space through K_+ , where the latter is transformed from a source (unstable

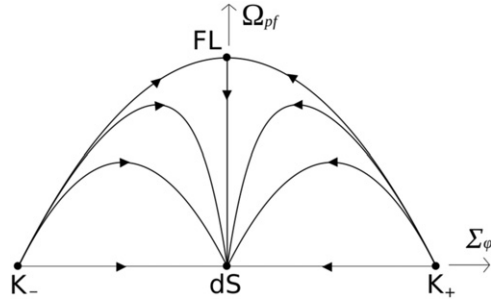


Figure 2. Orbit structure for a perfect fluid and a constant scalar field potential and hence $\lambda = 0$. The heteroclinic orbit $FL \rightarrow dS$, which is the unstable manifold of FL and also a separatrix in the state space $(\Sigma_\varphi, \Omega_{pf})$, yields the Λ CDM model when $\gamma = 1$.

node) to a saddle, with no orbits entering the interior state space. Finally, K_- is a source for all regions (and their bifurcation boundaries), while FL is a saddle, with a single orbit entering the interior state space, where S coalesce with FL in the limit $\lambda \rightarrow \infty$.

2.5. Center manifold analysis of the non-hyperbolic fixed points

Locally it remains to establish what happens near the fixed points P/S and K_+/P at the bifurcation values $\gamma = \lambda^2/3$ and $\lambda = \sqrt{6}$, respectively. In these cases one of the eigenvalues is zero. To establish what is happening locally therefore requires a center manifold analysis.

The linearisation around P/S yields the tangent spaces

$$E^s = \{(\Sigma_\varphi, \Omega_{pf}) | \Omega_{pf} = 0\}, \quad (16a)$$

$$E^c = \left\{(\Sigma_\varphi, \Omega_{pf}) \mid \left(\Sigma_\varphi - \frac{\lambda}{\sqrt{6}}\right) + \frac{\lambda}{\sqrt{6}} \Omega_{pf} = 0\right\}, \quad (16b)$$

where E^s is the stable tangent space spanned by the eigenvector associated with the negative eigenvalue $-\frac{1}{2}(6 - \lambda^2)$, with the $\Omega_{pf} = 0$ axis being the invariant stable manifold W^s , while E^c is the center tangent space associated with the zero eigenvalue. To study the stability associated with the zero eigenvalue we make use of the center manifold reduction theorem (see e.g. [33] section 2.12). Adapting the variables to E^s and E^c according to

$$(u, v) = \left(\left(\Sigma_\varphi - \frac{\lambda}{\sqrt{6}}\right) + \frac{\lambda}{\sqrt{6}} \Omega_{pf}, \Omega_{pf}\right) \quad (17)$$

result in that (11) yields a dynamical system on the form

$$u' = -\left(3 - \frac{\lambda^2}{2}\right)u + \mathcal{O}(\|(u, v)\|^2), \quad v' = \mathcal{O}(\|(u, v)\|^2), \quad (18)$$

where the fixed point P/S is located at the origin $(u, v) = (0, 0)$. The analytical one-dimensional center manifold W^c can be represented locally as the graph $h: E^c \rightarrow E^s$, where $u = h(v)$ satisfies the fixed point and tangency conditions $h(0) = 0$ and $\frac{dh}{dv}|_{v=0} = 0$, respectively. Inserting $u = h(v)$ into (18) and using v as the independent variable leads to

$$\left[2(1 + q) - \lambda^2\right]v \left(\frac{dh}{dv} - \frac{\lambda}{\sqrt{6}}\right) + (2 - q)g(v) - \sqrt{\frac{3}{2}}\lambda(1 - v - g^2(v)) = 0, \quad (19)$$

where

$$g(v) \equiv \frac{\lambda}{\sqrt{6}}(1-v) + h(v), \quad q = -1 + 3g^2(v) + \frac{\lambda^2}{2}v. \quad (20)$$

This equation can be solved approximately by representing $h(v)$ as the formal power series

$$h(v) = \sum_{i=2}^n a_i v^i + \mathcal{O}(v^{n+1}) \quad \text{as } v \rightarrow 0. \quad (21)$$

Inserting the above into (19) and solving algebraically for the coefficients leads to that on the center manifold

$$v' = -\lambda^2 v^2 + \mathcal{O}(v^3) \quad \text{as } v \rightarrow 0, \quad (22)$$

which shows that the fixed point P/S is stable. Thus a one-parameter family of orbits converge to P/S as $N \rightarrow +\infty$, tangentially to the center subspace E^c . In terms of the original state-space variables $(\Sigma_\varphi, \Omega_{\text{pf}})$ the analytical center manifold expansion gives

$$\Sigma_\varphi = \frac{\lambda}{\sqrt{6}} \left(1 - \Omega_{\text{pf}} + \frac{\lambda^2}{\lambda^2 - 6} \Omega_{\text{pf}}^2 + \mathcal{O}(\Omega_{\text{pf}}^3) \right) \quad \text{as } \Omega_{\text{pf}} \rightarrow 0. \quad (23)$$

It remains to analyze the bifurcation fixed point K_+/P . This turns out to be trivial since the center manifold of K_+/P is the $\Omega_{\text{pf}} = 0$ axis, which is also a one-dimensional unstable manifold of K_- . It follows that K_+/P is a saddle, for which no interior orbits converge to or originate from.

3. Global dynamical systems analysis

In this section we first present monotonic functions that completely determine the global solution structure of the present models. We then give an alternative proof for the global dynamics by means of a Dulac function.

3.1. Monotonic functions

We here use the methods developed in chapter 10 in [3] and then generalized in [22, 23] to derive monotonic functions that determine the global behavior of the solution space of the present set of models. The fixed point P/dS is stable when $\gamma > \lambda^2/3$ (region I) while the fixed point S is stable when $\gamma < \lambda^2/3$ (regions II and III and their mutual boundary at $\lambda = \sqrt{6}$). For each of these two cases, and for $\gamma = \lambda^2/3$, there exists a monotonic function associated with the stable fixed point.

We begin with the first case, i.e., region I where $\gamma > \lambda^2/3$ and P/dS is stable. We also include the bifurcation boundary $\lambda^2 = 3\gamma$ where S enter the state space at P. Below we will prove the following theorem:

Theorem 3.1. *Global interior dynamics when $\gamma \geq \lambda^2/3$.*

- (a) *All interior orbits end at P (dS when $\lambda = 0$, P/S when $\gamma = \lambda^2/3$).*
- (b) *A single interior orbit originates from FL.*
- (c) *All remaining interior orbits originate from K_- and K_+ , each being a source for a one-parameter set of interior orbits.*

Remark 3.1. Recall that $\Omega_V > 0$ and $\Omega_{\text{pf}} > 0$ for interior orbits. For a visual representation of the global orbit structure, see figure 3(a).

Proof. Using the methods in [22, 23] we derive the following monotonic function for region I:

$$M \equiv (1 - u\Sigma_\varphi)^2 \Omega_V^{-1}, \quad u \equiv \frac{\lambda}{\sqrt{6}} < 1, \quad (24)$$

which is strictly monotonically decreasing for all interior orbits since

$$M' = - \left(\frac{6(\Sigma_\varphi - u)^2 + (3\gamma - \lambda^2)\Omega_{\text{pf}}}{1 - u\Sigma_\varphi} \right) M < 0, \quad (25)$$

where M takes its minimum value, $M = 1 - u^2$, at P/dS. Thus all interior orbits end at P/dS. Going backwards in time $M \rightarrow \infty$, which implies that $\Omega_V \rightarrow 0$. Taking the boundary structure into account together with the local fixed point analysis shows that one orbit originates from FL while all other interior orbits originate from the fixed points K_- and K_+ .

The bifurcation value $\gamma = \lambda^2/3$ yields

$$M' = - \left(\frac{6(\Sigma_\varphi - u)^2}{1 - u\Sigma_\varphi} \right) M \leq 0, \quad (26a)$$

$$M''|_{\Sigma_\varphi=u} = 0, \quad (26b)$$

$$M'''|_{\Sigma_\varphi=u} = -108\Omega_{\text{pf}}^2 u^2 (1 - u^2)^3 \Omega_V^{-1}, \quad \Omega_V = 1 - u^2 - \Omega_{\text{pf}}. \quad (26c)$$

As a consequence $M' < 0$ when $\Sigma_\varphi \neq u$. Furthermore, as follows from (26c), when $\Sigma_\varphi = u$ interior orbits only go through an inflection point since $\Omega_{\text{pf}} > 0$ (i.e., there is no invariant interior set with $\Omega_{\text{pf}} > 0$, $\Sigma_\varphi = u$). Thus $M \rightarrow 1 - u^2$ toward the future with the limit at P/S, while $M \rightarrow \infty$ and hence $\Omega_V \rightarrow 0$ toward the past also in this case. Combining this with the boundary structure and the local analysis of the hyperbolic fixed points FL, K_\pm and the center manifold analysis of P/S yield the same result as when $\gamma > \lambda^2/3$, which concludes the proof of theorem 3.1. \square

Theorem 3.2. *Global interior dynamics when $\gamma < \lambda^2/3$.*

- (a) *All interior orbits end at S.*
- (b) *A single interior orbit originates from FL.*
- (c) *A one-parameter set of interior orbits originate from K_- .*
- (d) *When $\lambda < \sqrt{6}$ there is also a one-parameter set of interior orbits that originates from K_+ , while a single interior orbit originates from P.*
- (e) *When $\lambda \geq \sqrt{6}$ all interior orbits apart from the single one from FL originate from K_- .*

Remark 3.2. For a visual representation of the global orbit structure, see figures 3(b) and (c).

Proof. Using the methods developed in chapter 10 in [3, 22, 23] result in the following monotonic function when S is stable:

$$M \equiv (1 - v\Sigma_\varphi)^2 \Omega_V^{a-1} \Omega_{\text{pf}}^{-a}, \quad v \equiv \sqrt{\frac{3}{2}} \left(\frac{\gamma}{\lambda} \right), \quad a \equiv \frac{2(\lambda^2 - 3\gamma)}{2\lambda^2 - 3\gamma^2}, \quad (27)$$

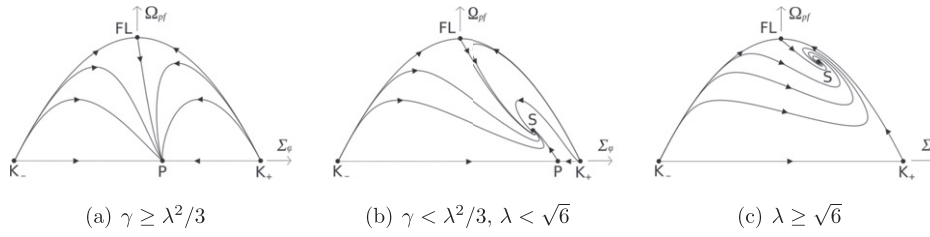


Figure 3. Orbit structure for a perfect fluid with linear equation of state $p_{\text{pf}} = (\gamma - 1)\rho_{\text{pf}}$ and an exponential/constant scalar field potential, $V = V_0 e^{-\lambda\varphi}$ for the three bifurcation regions I, II, III and their mutual boundaries at $\gamma = \lambda^2/3$, where P and S coincide, and $\lambda = \sqrt{6}$, where P coincide with K_+ .

where $0 < v < 1$ is the value of Σ_φ at the fixed point S, and where we note that $0 < a < 1$ when $\gamma < \lambda^2/3$; thus, the two exponents of Ω_V and Ω_{pf} are thereby negative. The e -fold time derivative of M is given by

$$M' = -\frac{3(2 - \gamma)(\Sigma_\varphi - v)^2 M}{(1 - v^2)(1 - v\Sigma_\varphi)} \leq 0, \quad (28)$$

where $M' = 0$ when $\Sigma_\varphi = v$, but then $M''|_{\Sigma_\varphi=v} = 0$ and

$$M'''|_{\Sigma_\varphi=v} = -\frac{27(2 - \gamma)[2v^2 - \gamma(1 - \Omega_{\text{pf}})]^2 M|_{\Sigma_\varphi=v}}{2v^2}, \quad (29)$$

where $M|_{\Sigma_\varphi=v} = (1 - v^2)\Omega_V^{a-1}\Omega_{\text{pf}}^{-a}$, $\Omega_V = 1 - v^2 - \Omega_{\text{pf}}$ and hence $M'''|_{\Sigma_\varphi=v} < 0$, except at the fixed point where $2v^2 - \gamma(1 - \Omega_{\text{pf}}) = 0$ and M is a constant and hence all its derivatives are zero, exemplified by that $M'''|_{\Sigma_\varphi=v}$ with $\Omega_{\text{pf}} = 1 - \frac{3\gamma}{\lambda^2}$ inserted yields zero. Thus M just goes through an inflection point for the interior orbits when $\Sigma_\varphi = v$, $\Omega_{\text{pf}} \neq 1 - \frac{3\gamma}{\lambda^2}$. To summarize: M is monotonically decreasing in the interior state space everywhere except at the fixed point S. As a consequence M decreases toward its positive minimum value at S for all interior orbits, and thus they all end at S. Furthermore, toward the past $M \rightarrow \infty$. Since both $a > 0$ and $a - 1 < 0$ this implies that $\Omega_V \rightarrow 0$ or/and $\Omega_{\text{pf}} \rightarrow 0$ toward the past for all interior orbits. It follows from the orbits on the boundaries $\Omega_V = 0$ and $\Omega_{\text{pf}} = 0$, and the local fixed point analysis, that there is one orbit entering the state space from the fixed point FL and one from P when $\lambda < \sqrt{6}$. The remaining interior orbits originate from the fixed point K_- only when $\lambda \geq \sqrt{6}$ and from both K_- and K_+ when $\lambda < \sqrt{6}$, each yielding one-parameter set of orbits. \square

This establishes the global solution structure for the present models for all $\lambda \geq 0$ and $\gamma \in (0, 2)$.¹² The solution structure is depicted in figure 3.

However, we here offer an alternative proof using a Dulac function instead of monotonic functions.

¹² For those that are so inclined, it is possible to formalize the above monotonicity arguments further with the *monotonicity principle*. The version on p 103 in [3] is as follows: let ϕ_t be a flow on \mathbb{R} with S an invariant set. Let $M : S \rightarrow \mathbb{R}$ be a C^1 function whose range is the interval (a, b) , where $a \in \mathbb{R} \cup \{-\infty\}$, $b \in \mathbb{R} \cup \{+\infty\}$ and $a < b$. If M is decreasing on orbits in S , then for all $\mathbf{x} \in S$, the ω - and α -limit sets of orbits in S are given by $\omega(\mathbf{x}) \subseteq \{s \in S \mid \lim_{y \rightarrow s} M(y) \neq b\}$ and $\alpha(\mathbf{x}) \subseteq \{s \in S \mid \lim_{y \rightarrow s} M(y) \neq a\}$, respectively. A more advanced version of the monotonicity principle can be found in appendix D in [34].

3.2. The Dulac function

In contrast to the previous direct proofs, the present one relies on the Poincaré–Bendixson theorem.

Theorem 3.3. *Global interior dynamics when $\gamma \in (0, 2)$.*

The global dynamics of the dynamical system (11) can be inferred from the local stability analysis of the fixed points.

Proof. The proof relies on the existence of a Dulac function and the simple boundary structure. Let $(\Sigma'_\varphi, \Omega'_{\text{pf}}) = (f_\Sigma, f_\Omega) = \vec{f}$, where f_Σ and f_Ω are the right-hand sides of (11a) and (11b), respectively. In contrast to monotonic functions we do not have a systematic method for obtaining Dulac functions. However, since they are less restrictive for the dynamics it seems natural to make the ansatz $\Omega_V^{-a} \Omega_{\text{pf}}^{-b}$. This gives

$$\begin{aligned} \nabla \cdot (\Omega_V^{-a} \Omega_{\text{pf}}^{-b} \vec{f}) &= \Omega_V^{-a} \Omega_{\text{pf}}^{-b} \left[\frac{3}{2}(5 - 2a - 2b)(\gamma \Omega_{\text{pf}} + 2\Sigma_\varphi^2) \right. \\ &\quad \left. + \sqrt{6}\lambda(a - 1)\Sigma_\varphi - 3(1 + \gamma - b\gamma) \right], \end{aligned} \quad (30)$$

where $\nabla = (\partial_{\Sigma_\varphi}, \partial_{\Omega_{\text{pf}}})$. Choosing $a = 1$ to eliminate the linear Σ_φ term and then $b = 3/2$ to eliminate the Ω_{pf} and Σ_φ^2 terms yield

$$\nabla \cdot (\Omega_V^{-1} \Omega_{\text{pf}}^{-3/2} \vec{f}) = -\frac{3}{2}(2 - \gamma)\Omega_V^{-1} \Omega_{\text{pf}}^{-3/2} < 0, \quad \gamma \in (0, 2), \quad (31)$$

i.e., the divergence of $\Omega_V^{-1} \Omega_{\text{pf}}^{-3/2} \vec{f}$ is strictly negative in the interior state space when $\gamma \in (0, 2)$.

The function $\Omega_V^{-1} \Omega_{\text{pf}}^{-3/2}$ is thereby a Dulac function, which excludes the possibility of interior periodic orbits, see e.g. p 265 in [33]. In combination with that there are no heteroclinic cycles on the boundary, it follows from the Poincaré–Bendixson theorem on \mathbb{R}^2 (see e.g. [33] section 3.7) that the only possible α - and ω -limit sets of the orbits (i.e., their future and past asymptotics) of the system (11) are the fixed points, i.e., the local analysis of the fixed points completely describes the future and past asymptotics of the dynamical system (11). \square

In conclusion: in contrast to earlier work, we have performed a complete local and global analysis on FLRW models with a minimally coupled scalar field with an exponential potential and a perfect fluid with a linear equation of state. This has been accomplished by complementing previous linear analysis of hyperbolic fixed points with a center manifold analysis of non-hyperbolic fixed points, associated with bifurcations, and by constructing monotonic functions and a Dulac function that subsequently were used to give a global description of the dynamics of these models. The present analysis and methods serve as a starting point for investigations of models with more general asymptotically exponential potentials, and also for inhomogeneous perturbations of such models, topics that we will come back to in future papers.

Acknowledgments

It is a pleasure to thank John Wainwright for many useful discussions and for suggesting that we write the present paper. A A is supported by FCT/Portugal through CAMGSD, IST-ID, projects UIDB/04459/2020 and UIDP/04459/2020.

Data availability statement

No new data were created or analysed in this study.

ORCID iDs

Artur Alho  <https://orcid.org/0000-0002-5753-8333>

Woei Chet Lim  <https://orcid.org/0000-0002-6422-4201>

Claes Uggla  <https://orcid.org/0000-0002-0906-8808>

References

- [1] Collins C B 1971 More qualitative cosmology *Commun. Math. Phys.* **23** 137–58
- [2] Bogoyavlenskii O I and Novikov S P 1973 Singularities of the cosmological model of the Bianchi IX type according to the qualitative theory of differential equations *J. Exp. Theor. Phys.* **37** 747–55
- [3] Wainwright J and Ellis G F R 1997 *Dynamical Systems in Cosmology* (Cambridge: Cambridge University Press)
- [4] Coley A A 2003 *Dynamical Systems and Cosmology* (Dordrecht: Kluwer)
- [5] Bahamonde S, Böhmer C G, Carloni S, Copeland E J, Fang W and Tamanini N 2018 Dynamical systems applied to cosmology: dark energy and modified gravity *Phys. Rep.* **775–777** 1–122
- [6] Belinskii V A, Grishchuk L P, Khalatnikov I M and Zeldovich Y B 1985 Inflationary stages in cosmological models with a scalar field *Sov. Phys. - JETP* **62** 195
- [7] Belinskii V A, Grishchuk L P, Khalatnikov I M and Zeldovich Y B 1985 Inflationary stages in cosmological models with a scalar field *Phys. Lett. B* **155** 232
- [8] Belinskii V A and Khalatnikov I M 1987 On the generality of inflationary solutions in cosmological models with a scalar field *Sov. Phys. - JETP* **66** 441
- [9] Belinskii V A, Ishihara H, Khalatnikov I M and Sato H 1988 On the degree of generality of inflation in Friedmann cosmological models with a massive scalar field *Prog. Theor. Phys.* **79** 676–84
- [10] Halliwell J J 1987 Scalar fields in cosmology with an exponential potential *Phys. Lett. B* **185** 341
- [11] Ratra B and Peebles P J E 1988 Cosmological consequences of a rolling homogeneous scalar field *Phys. Rev. D* **37** 3406
- [12] Coley A A, Ibáñez J and van den Hoogen R J 1997 Homogeneous scalar field cosmologies with an exponential potential *J. Math. Phys.* **38** 17
- [13] Foster S 1998 Scalar field cosmologies and the initial spacetime singularity *Class. Quantum Grav.* **15** 3485
- [14] Copeland E J, Liddle A R and Wands D 1998 Exponential potentials and cosmological scaling solutions *Phys. Rev. D* **57** 4686
- [15] Foster S 1998 Scalar field cosmological models with hard potential walls (arXiv:gr-qc/9806113)
- [16] Uggla C 2013 Spacetime singularities: recent developments *Int. J. Mod. Phys. D* **22** 1330002
- [17] Carr B J, Coley A A, Goliath M, Nilsson U S and Uggla C 2000 Critical phenomena and a new class of self-similar spherically symmetric perfect-fluid solutions *Phys. Rev. D* **61** 081502
- [18] Zhang X and An X 2015 Naked singularity and black hole formation in self-similar Einstein-scalar fields with exponential potentials (arXiv:1509.07954)
- [19] Uggla C, Jantzen R T and Rosquist K 1995 Exact hypersurface-homogeneous solutions in cosmology and astrophysics *Phys. Rev. D* **51** 5522
- [20] Uggla C 2013 Recent developments concerning generic spacelike singularities *Gen. Relativ. Gravit.* **45** 1669–710
- [21] Lim W C, van Elst H, Uggla C and Wainwright J 2004 Asymptotic isotropization in inhomogeneous cosmology *Phys. Rev. D* **69** 103507
- [22] Heinzle J M and Uggla C 2010 Monotonic functions in Bianchi models: why they exist and how to find them *Class. Quantum Grav.* **27** 015009
- [23] Hervik S, Lim W C, Sandin P and Uggla C 2010 Future asymptotics of tilted Bianchi type II cosmologies *Class. Quantum Grav.* **27** 185006
- [24] Alho A and Uggla C 2015 Scalar field deformations of Λ CDM cosmology *Phys. Rev. D* **92** 103502

- [25] Ureña-López L A 2012 Unified description of the dynamics of quintessential scalar fields *J. Cosmol. Astropart. Phys.* **JCAP03(2012)035**
- [26] Tsujikawa S 2013 Quintessence: a review *Class. Quantum Grav.* **30** 214003
- [27] Anzai H 1951 Ergodic skew product transformations on the torus *Osaka Math. J.* **3** 83
- [28] Alho A and Uggla C 2015 Global dynamics and inflationary center manifold and slow-roll approximants *J. Math. Phys.* **56** 012502
- [29] Alho A, Hell J and Uggla C 2015 Global dynamics and asymptotics for monomial scalar field potentials and perfect fluids *Class. Quantum Grav.* **32** 145005
- [30] Alho A and Uggla C 2017 Inflationary α -attractor cosmology: a global dynamical systems perspective *Phys. Rev. D* **95** 083517
- [31] Alho A, Uggla C and Wainwright J 2021 Quintessence (in preparation)
- [32] Joyce M and Prokopec T 1998 Turning around the sphaleron bound: electroweak baryogenesis in an alternative post-inflationary cosmology *Phys. Rev. D* **57** 6022–49
- [33] Perko L 2000 *Differential Equation and Dynamical Systems* 3rd edn (*Texts in applied mathematics* vol 7) (New York: Springer)
- [34] Fjällborg M, Heinzle J M and Uggla C 2007 Self-gravitating stationary spherically symmetric systems in relativistic galactic dynamics *Math. Proc. Camb. Phil. Soc.* **143** 731